THE UNIVERSITY *of* EDINBURGH

Edinburgh Research Explorer

Experimental Demonstration of Subband Index Techniques for m-CAP in Short Range SI-POF Links

OPEN ACCESS

Experimental Demonstration of Subband Index Techniques for m-CAP in Short Range SI-POF Links

Kabiru O. Akande, *Student Member, IEEE* and Wasiu O. Popoola, *Senior Member, IEEE*

Abstract—In this letter, novel spectrally-efficient subband index (SI) techniques have been developed for multiband carrierless amplitude and phase modulation (m-CAP). The subband index techniques transmit additional information bit on the index of the conventional m-CAP subbands. Experimental demonstrations are performed in a short range optical data link using step-index plastic optical fibre (SI-POF). The demonstrations show that the proposed techniques enable flexibility in design and significantly improve the power/spectral efficiency of the conventional m-CAP.

Index Terms—Optical communication, step-index plastic optical fibre (SI-POF), index modulation, multiband carrierless amplitude phase modulation (m-CAP).

I. Introduction

Multiband carrierless amplitude and phase modulation (m-CAP) has been proposed for overcoming the bandwidth limitation in short-range plastic optical fibre (POF) communication systems and improving the achievable capacity [1]. The single wide-band of CAP is divided into multiple narrow bands to realize m-CAP scheme. This gives m-CAP scheme the flexibility of adapting the transmitted signal to the channel state conditions and substantially improving the bit error rate (BER) performance of CAP [1].

However, both m-CAP and CAP have the same spectral efficiency. Staggered CAP has been proposed in [2] for achieving a 100% spectral efficiency in CAP. Similarly, in this letter, novel subband index CAP (SI-CAP) techniques that enhance the spectral efficiency of the conventional m-CAP are proposed and experimentally demonstrated. In SI-CAP, the subbands of a conventional m-CAP are divided into two groups: the active and inactive subbands [3]. The active subbands are modulated with M-QAM data symbols while the inactive subbands are nulled, that is they carry no data at all. The SI-CAP encodes additional information bits in the selection (i.e. indexing) of which subbands to make active. This way, the SI-CAP provides design flexibility that enables adaptive trade-off between the power and spectral efficiency of the conventional m-CAP.

The challenge in SI-CAP is that the number of subbands required to achieve the same spectral efficiency as m-CAP increases as the constellation size, M, increases. This requirement results in increased complexity for SI-CAP for large constellation sizes [3]. Consequently, an enhanced SI-CAP (eSI-CAP) which employs a dual constellation is developed to address this problem. The concept of using dual constellation has been proposed by [4] for orthogonal frequency division multiplexing (OFDM) and is implemented in this work to improve the m-CAP performance. In contrast

to SI-CAP which nulls the inactive subbands by carrying no data symbols on them, eSI-CAP modulates them using symbols from a constellation other than the one employed for the active subbbands. As a result, eSI-CAP utilizes a dual distinguishable constellation $\mathcal{M}_\mathrm{A}$ and $\mathcal{M}_\mathrm{B}$ such that $\mathcal{M}_\mathrm{A} \cap \mathcal{M}_\mathrm{B} = \emptyset$ and $\mathcal{M}_\mathrm{A} \cup \mathcal{M}_\mathrm{B} = \mathcal{M}$. Thus, in addition to the index bits, the eSI-CAP modulates the active and the inactive subbands with symbols from $\mathcal{M}_\mathrm{A}$ and $\mathcal{M}_\mathrm{B}$, respectively [4]. Therefore, eSI-CAP enhances the spectral efficiency of m-CAP for any number of subbands and constellation sizes without increasing the complexity of the resulting system.

Furthermore, a novel detection scheme is developed for the subband index schemes that achieves maximum likelihood solution but with the same order of complexity as the conventional m-CAP modulation. Thus, the benefits of the developed subband index schemes are accessible without much increase in system complexity. The performance of the subband index schemes are experimentally demonstrated for a short optical data link using step-index plastic optical fibre (SI-POF). The SI-POF is very attractive for short range optical communication due to its ease of handling and installation which lowers the overall cost of implementation. The experimental demonstrations in SI-POF show that for a fixed power efficiency, the SI-CAP schemes achieve higher spectral efficiency in comparison to the conventional m-CAP.

The main contributions of this letter are summarized as follows: 1.) Spectrally-efficient subband index schemes are experimentally demonstrated to improve the spectral efficiency and BER of an m-CAP based short range POF communication link; 2.) a low complexity detector that achieves the maximum likelihood solution is developed for the subband index modulation schemes. The rest of the paper is organized as follows: the system models for the subband index schemes are presented in Section II. The detection schemes are detailed in Section III while Section IV describes the experimental demonstration and discusses the results. Section V concludes the paper.

II. System Model for the Subband Index Schemes

For completeness, brief description of the conventional m-CAP scheme is first illustrated after which the subband index schemes are presented.

A. Brief illustration of m-CAP

The m-CAP signal is realized by mapping stream of information bits to M-QAM constellation symbols. The symbols are upsampled, separated into real and imaginary parts and respectively passed through in-phase ($h(t)$) and quadrature ($\bar{h}(t)$) transmit filters [2]. The filters form a Hilbert

The Authors are with the School of Engineering, Institute for Digital Communications, LiFi Research and Development Centre, The University of Edinburgh, Edinburgh, UK (email: {K.Akande,W.Popoola}@ed.ac.uk).
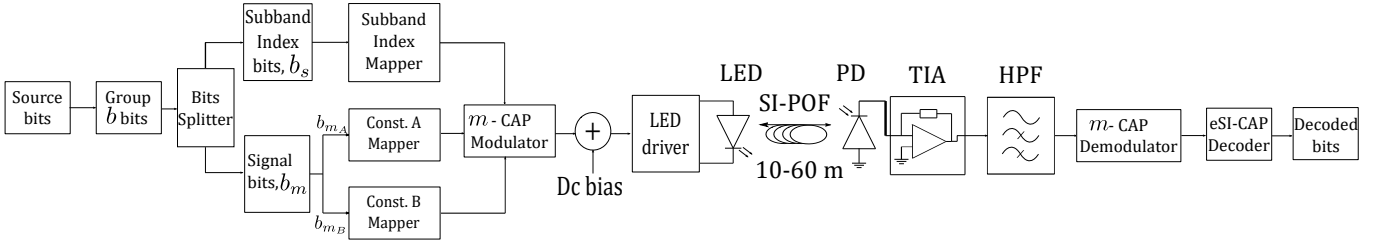
Fig. 1. The schematic block diagram of the eSI-CAP for short range SI-POF communication link.

TABLE I
MAPPING PROCESS FOR THE PROPOSED eSI-CAP WITH
$N = 4$, $N_a = 2$ AND $M = 4$

b_s bits	$S = [S_A; S_B]$	$\log_2(M)$ bits	$\mathcal{M}_A$	$\mathcal{M}_B$
00	$[1, 2; 3, 4]$	00	$+1 + j$	$+(1 + \sqrt{3})$
01	$[1, 3; 2, 4]$	01	$-1 + j$	$+j(1 + \sqrt{3})$
10	$[1, 4; 2, 3]$	10	$-1 - j$	$-(1 + \sqrt{3})$
11	$[2, 3; 1, 4]$	11	$+1 - j$	$-j(1 + \sqrt{3})$

pair and are realised, for each of the N subbands of m-CAP, as:

$$h_n(t) = g(t)\cos(2\pi f_{c,n} t) \tag{1}$$

and

$$\bar{h}_n(t) = g(t)\sin(2\pi f_{c,n} t) \tag{2}$$

where $g(t)$ is the root raised cosine filter (RRCF) and $f_{c,n}$ is the center frequency of the nth subband and expressed as:

$$f_{c,n} = (2n - 1)f_c, \quad n = 1, 2, \cdots, N \tag{3}$$

to achieve orthogonality between the subbands of m-CAP. The outputs of the filters are added together with a DC-bias to ensure non-negativity. The resulting signal is used to modulate an optical source and sent through the SI-POF channel. At the receiver, a photodiode (PD) converts the incoming optical intensity to a current signal, this is further converted to a voltage signal by the transimpedance amplifier (TIA) and passed through a high-pass filter (HPF) to remove any DC component. The signal is then demodulated using a reversed and conjugated version of the transmit filters. Thereafter, it is mapped to the corresponding bits using M-QAM decoder.

B. Model Description for the Subband Index Schemes

Detailed description of the eSI-CAP model is first presented and from this, the SI-CAP can be obtained as a special case. The block diagram of the proposed eSI-CAP is shown in Fig. 1. The information bits are first grouped in blocks of b bits and are further divided into subband index bits, b_s, and signal bits, b_m. The b_s bits are used to select or activate N_a 'active' subbands that will be modulated with symbols from $\mathcal{M}_A$. The remaining N_b 'inactive' subbands will be modulated with symbols from $\mathcal{M}_B$. Thus, the total number of transmitted signal bits, $b_m = N_a\log_2(M_A) + N_b\log_2(M_B)$ where M_A and M_B are the sizes of $\mathcal{M}_A$ and $\mathcal{M}_B$, respectively.

The choice of $\mathcal{M}_A$ and $\mathcal{M}_B$ plays an important role in determining the BER performance of eSI-CAP. Constellation points within the combined $\mathcal{M}_A \cup \mathcal{M}_B$ should have similar minimum Euclidean distance (MED) as those of either $\mathcal{M}_A$ or $\mathcal{M}_B$. To achieve this goal, the constellation can be jointly designed before being separated into its constituent parts. Considering an average power constraint, the optimum constellation points for the configuration considered in this work (for $M_A = M_B = 4$) are given in Table I [5]. The MED of the constellation is higher than that of the corresponding rectangular QAM constellation under an average power constraint. Hence, the constellation is adopted in this work.

As an example, the mapping process for the eSI-CAP is illustrated for a total of $N = 4$ subbands, number of active subbands, $N_a = 2$ and constellation sizes $M_A = M_B = 4$ as follows: there are ${}^N C_{N_a} = 6$ ways of selecting the N_a active subbands. Any $N_u = 2^{\lfloor \log_2 {}^N C_{N_a} \rfloor} = 4$ of these 6 combinations can then be used for the subband index bits, $b_s = \log_2(N_u)$. If bits $b = $ '0110010111' is to be transmitted, then the first b_s bits, '01', is mapped to the corresponding subband selection, $S_2 = [1, 3; 2, 4]$ as Table I shows. This means that subbands 1 and 3 are activated and will be modulated from $\mathcal{M}_A$ while subbands 2 and 4 are modulated from $\mathcal{M}_B$. The next $N_a\log_2(M_A)$ bits, '1001', are used to draw symbols $-1 - j$ and $-1 + j$ from $\mathcal{M}_A$ for transmission on the active subbands 1 and 3, respectively. While the last $N_b\log_2(M_B)$ bits, '0111', are used to draw symbols $+j(1 + \sqrt{(3)})$ and $-j(1 + \sqrt{(3)})$ from $\mathcal{M}_B$ for transmission on the remaining subbands 2 and 4, respectively. The resulting eSI-CAP signal vector that is sent to the m-CAP modulator is given as:

$$\mathbf{x} = \begin{bmatrix} -1 - j & +j(1 + \sqrt{3}) & -1 + j & -j(1 + \sqrt{3}) \end{bmatrix}^T. \tag{4}$$

The mapping process illustrated above is the same for configurations employing $M > 4$, except that the constellation will be different. Some candidate constellations are reported in [4, 5]. A special case of eSI-CAP, in which only the active subbands carry constellation symbols while the rest are nulled, is termed SI-CAP. That is, subbands 2 and 4 in the example above will be null and set to zero [3].

The transmission efficiency, defined as the number of bits per symbol divided by the number of subbands, of eSI-CAP is expressed as:

$$\mathcal{T}_{\text{eSI-CAP}} = \frac{\lfloor \log_2 \left({}^N C_{N_a} \right) \rfloor + N_a\log_2(M_A) + N_b\log_2(M_B)}{N} \tag{5}$$

Algorithm 1 LCD Algorithm
───────────────────────────────
Require: $\mathbf{y}, \mathbf{h}, \mathcal{M}_A, M_A, N, N_a, N_b$
Ensure: $\mathcal{S}_A$ and $\mathcal{S}_B$ are the active and inactive subband indices, respectively;
  Initialization:
1: $\boldsymbol{\chi} = \{\chi_{m_a}\}_{m_a=1}^{M_A}$; $\boldsymbol{\lambda} = \{\lambda_n\}_{n=1}^{N}$; $\{s_{m_a}\}_{m_a=1}^{M_A} = \mathcal{M}_A$;
  Note: $\{\chi_{m_a}\}_{m_a=1}^{M_A} \Rightarrow \begin{bmatrix} \chi_1 & \chi_2 \cdots \chi_{M_A} \end{bmatrix}$ and so on.
  Recursion:
2: **for** $(n = 1; n \leq N; n++)$ **do**
3:   **for** $(m_a = 1; m_a \leq M_A; m_a++)$ **do**
4:     $\chi_{m_a} = |y_n - h_n s_{m_a}|^2$;
5:   **end for**
6:   $\lambda_n = \min_{m_a}\{\chi_{m_a}\}_{m_a=1}^{M_A}$;
7: **end for**
8: $\bar{\boldsymbol{\lambda}} = \{\bar{\lambda}_n\}_{n=1}^{N} = sort(\boldsymbol{\lambda})$, $\{sort(\cdot)$ arranges the elements of $(\cdot)$ in an increasing order and returns their corresponding indices$\}$;
9: $\mathcal{S}_A = \{\bar{\lambda}_{n_a}\}_{n_a=1}^{N_a}$;
10: $\mathcal{S}_B = \{\bar{\lambda}_{N-N_b+n_b}\}_{n_b=1}^{N_b}$;
11: **return** $\mathcal{S}_A, \mathcal{S}_B$;
───────────────────────────────

Fig. 2. Illustration of the set-up for the experimental demonstration with SI-POF link.

while that of SI-CAP is given as [3]:

$$\mathcal{T}_{\text{SI-CAP}} = \frac{\lfloor \log_2\left(^{N}C_{N_a}\right)\rfloor + N_a\log_2(M)}{N}. \tag{6}$$

As for $\mathcal{T}_{m-\text{CAP}}$, it is $\log_2(M)$ irrespective of the N employed. It can therefore be concluded that the proposed subband index schemes improve the transmission efficiency of the conventional m-CAP and enable design flexibility.

III. DETECTION TECHNIQUES

The received electrical signal at the output of the m-CAP demodulator can be represented as:

$$\mathbf{y} = \Re\mathcal{K}\beta\mathbf{h}\mathbf{x} + \mathbf{w} \tag{7}$$

where y_n, h_n, x_n and w_n are the components of $N \times 1$ vectors $\mathbf{y}$, $\mathbf{h}$, $\mathbf{x}$ and $\mathbf{w}$, respectively. The $\Re$ represents PD responsivity, $\mathcal{K}$ represents the electrical to optical conversion coefficient, β is the modulation index while h_n and w_n respectively represent SI-POF attenuation and the noise sample for the n_{th} subband. By letting $\mathbf{r} = \Re\mathcal{K}\beta\mathbf{h}\mathbf{x}$, the expression in (7) can be written as:

$$\mathbf{y} = \mathbf{r} + \mathbf{w}. \tag{8}$$

The optimum receiver for eSI-CAP is the maximum likelihood detector (MLD) [3]. However, the MLD considers all possible $N_u M_A^{N_a} M_B^{N_b}$ combinations of $\mathbf{r}$ when making decisions. Thus, MLD becomes computationally infeasible for increasing constellation sizes.

As a result, a lower complexity detector (LCD) that achieves the same solution as the MLD is developed for the subband index schemes. The LCD is elucidated in Algorithm 1. From Algorithm 1, it is seen that the complexity of the LCD is linear with order $\mathcal{O}(NM)$ compared to that of MLD, which grows exponentially with order $N_u M_A^{N_a} M_B^{N_b}$. Using the outputs of Algorithm 1, the symbols on the active and inactive subbands
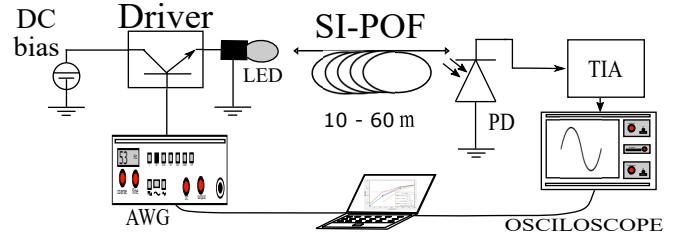
can easily be detected by mapping them to the nearest symbol in $\mathcal{M}_A$ and $\mathcal{M}_B$, respectively.

IV. EXPERIMENTAL RESULTS AND DISCUSSIONS

The set-up for the experimental demonstration with an SI-POF link is depicted in Fig. 2. The values of the filter parameters specified in [1] are employed for the three schemes. The signals corresponding to each of the schemes is generated on a computer before being sent to an arbitrary waveform generator (AWG, Agilent 33600 series). The continuous waveform from the AWG is fed to the LED driver with an added suitable DC bias before being used to modulate the intensity of the resonant-cavity LED [3]. The optical signal is transmitted through the SI-POF (HFBR-RUD500Z) and received by a PIN-based photo-receiver (PDA10A). A digital oscilloscope (Agilent 7000B Series) is used to capture the received electrical signal, followed by an offline post-detection processing. The response of the link can be approximated as a 4$^{\text{th}}$ order low-pass filter with a measured 3 dB bandwidth of 100 MHz. The system sampling rate is 500 MSa/s. The results are presented using the 'link spectral efficiency', defined as the bit rate divided by the link's 3 dB bandwidth.

The selection of the optimum power-efficient configuration for eSI-CAP at a fixed $\mathcal{T}$ is illustrated in Fig. 3 in 10 m SI-POF link for different modulation index, β. Multiple configurations of eSI-CAP with the same $\mathcal{T}$ have different BER performance due to the use of dual distinct constellations. Using $N = 16$ and $M = 4$, the eSI-CAP configurations with $N_a = 1$ and 15 have the same $\mathcal{T} = 2.25$. However, as shown in Fig. 3 at BER of 3×10^{-3} and $\beta = 0.36$, the configuration with $N_a = 15$ achieves spectral efficiency, η, of 5.58 bit/s/Hz in comparison to 5.3 bit/s/Hz achieved with $N_a = 1$. This leads to a η gain of 0.48 bit/s/Hz which increases to 0.55 bit/s/Hz at β of 0.48. Thus, it is found that for a fixed $\mathcal{T}$, the configuration with the highest N_a has the best BER performance and hence is the most power efficient. As a result, the configuration with $N_a = 15$ has been adopted for eSI-CAP in subsequent results.

The BER performance of the subband index schemes are compared to that of the conventional m-CAP in Fig. 4 using $N = 16$ and $N_a = 15$ in 10 m SI-POF link. The figure shows the performance advantage of the subband index schemes over m-CAP and depicts the enhancement of SI-CAP by eSI-CAP. For example, at a BER of 3×10^{-3} and $\beta = 0.12$, eSI-CAP achieves η of 5.05 bit/s/Hz in comparison to 4.85 bit/s/Hz and 4.55 bit/s/Hz achieved by SI-CAP and m-CAP, respectively. Thus, eSI-CAP has a η gain
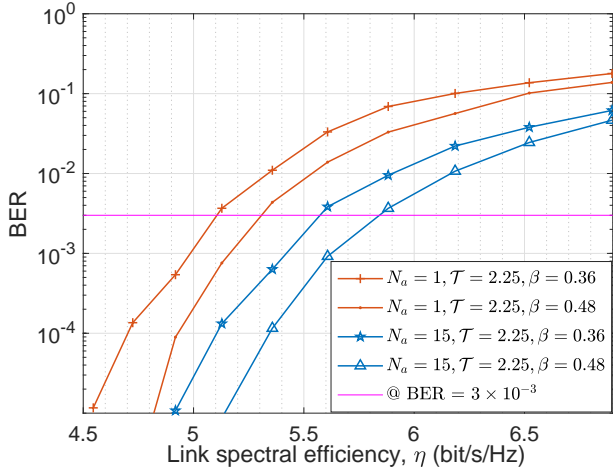
Fig. 3. Optimum power-efficient configuration for enhanced subband index CAP (eSI-CAP) at a fixed transmission efficiency ($\mathcal{T}$) with different modulation index (β), $N = 16$, $N_{\mathrm{a}} = [1, 15]$, $M = 4$ and $\beta = [0.48, 0.36]$.
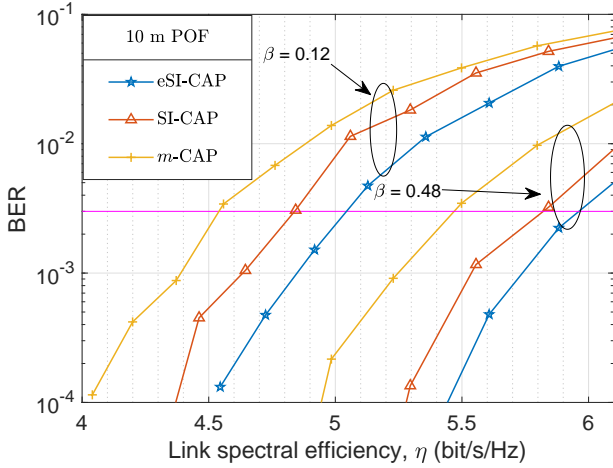

Fig. 4. Performance comparison of the subband index schemes and m-CAP at different modulation index, β using $N = 16$ and $N_{\mathrm{a}} = 15$ in 10 m SI-POF link.
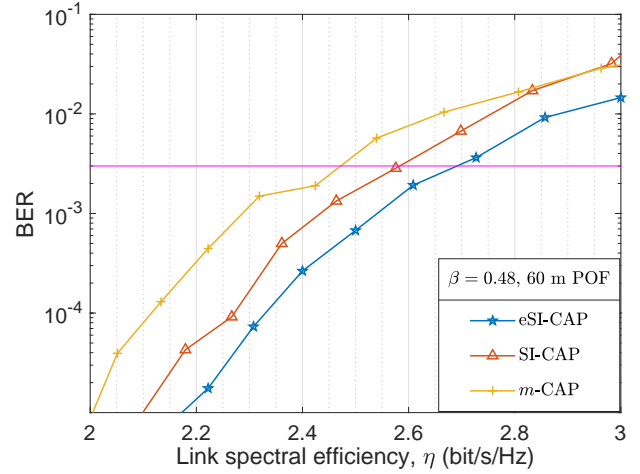

Fig. 5. Performance comparison of the subband index schemes and m-CAP with $\beta = 0.48$, $N = 16$ and $N_{\mathrm{a}} = 15$ in 60 m SI-POF link.

TABLE II
THE SPECTRAL EFFICIENCY ACHIEVED BY EACH SCHEME BELOW THE FEC BER LIMIT OF 3×10^{-3} WITH DIFFERENT MODULATION INDEX (β), $N = 16$ AND $N_{\mathrm{a}} = 15$.

Scheme \ β	0.48	0.36	0.24	0.12	0.06
$\eta_{\mathrm{eSI\text{-}CAP}}$ (bit/s/Hz)	5.97	5.78	5.57	5.05	4.3
$\eta_{\mathrm{SI\text{-}CAP}}$ (bit/s/Hz)	5.83	5.52	5.28	4.85	4.05
$\eta_{m\text{-}CAP}$ (bit/s/Hz)	5.42	5.28	4.98	4.55	3.83

2.47 bit/s/Hz achieved by SI-CAP and m-CAP, respectively. It is therefore concluded that the proposed subband index schemes significantly improve the spectral/power efficiency of the conventional m-CAP in short range optical data links.

V. CONCLUSION

Novel subband index (SI) schemes that improve the power/spectral efficiency of the conventional m-CAP have been developed. A low complexity detector (LCD) that achieves maximum likelihood solution is also developed for the subband index schemes. It is shown, through experimental demonstrations in 10 m and 60 m SI-POF links, that for a fixed power spectral efficiency, the subband index schemes achieves higher spectral efficiency in comparison to the conventional m-CAP and vice versa. Therefore, the proposed schemes are suitable for short range optical data communications due to their design flexibility and superior spectral/power efficiency over the conventional m-CAP scheme.

of 0.2 bit/s/Hz and 0.5 bit/s/Hz over SI-CAP and m-CAP, respectively. When the β is increased to 0.48 at the same BER, eSI-CAP maintains its performance advantage as it achieves η gain of 0.14 bit/s/Hz and 0.5 bit/s/Hz over SI-CAP and m-CAP, respectively. Alternatively, if the η is fixed at 5.6 bit/s/Hz for all the schemes at $\beta = 0.48$, the eSI-CAP and SI-CAP achieve BER of 5×10^{-4} and 1.5×10^{-3} respectively in comparison to 5×10^{-3} achieved by m-CAP. Thus, the proposed subband index schemes achieve better spectral efficiency for a fixed power efficiency and vice versa when compared with the conventional m-CAP. It can be seen from Table II that the subband index schemes consistently outperform the conventional m-CAP over all the range of β investigated and that eSI-CAP maintains its performance enhancement of SI-CAP over these range.

Finally, the performance enhancement of the subband index schemes is validated for longer SI-POF link of 60 m as shown in Fig. 5. At BER of 3×10^{-3} and $\beta = 0.48$, the eSI-CAP achieves η of 2.7 bit/s/Hz in comparison to 2.55 bit/s/Hz and

REFERENCES

[1] M. I. Olmedo *et al.*, "Multiband carrierless amplitude phase modulation for high capacity optical data links," *Journal of Lightwave Technology*, vol. 32, no. 4, pp. 798–804, Feb 2014.
[2] G. Stepniak, "Staggered CAP - A new spectrally efficient modulation format for optical communications," *IEEE Photonics Technology Letters*, vol. 30, no. 4, pp. 367–370, Feb 2018.
[3] K. O. Akande and W. O. Popoola, "Subband index carrierless amplitude and phase modulation for optical communications," *Journal of Lightwave Technology*, vol. 36, no. 18, pp. 4190–4197, Sept 2018.
[4] T. Mao, Z. Wang, Q. Wang, S. Chen, and L. Hanzo, "Dual-mode index modulation aided OFDM," *IEEE Access*, vol. 5, pp. 50–60, 2017.

[5] G. Foschini *et al.*, "Optimization of two-dimensional signal constellations in the presence of Gaussian noise," *IEEE Transactions on Communications*, vol. 22, no. 1, pp. 28–38, January 1974.